Ultrafast Phase Aberration Correction in Ultrasound Imaging Using a Simple Model for Fat Layer

Ahmed M. Ehab*, Zyad Farouk, Abou-Bakr M. Youssef, and Yasser M. Kadah

Biomedical Engineering Department, Cairo University, Egypt

Abstract– This paper presents a computationally efficient method to correct the phase aberration problem arises from the subcutaneous fat layer. The method is based on the determination of thickness of the fat layer to calculate the focusing delay perfectly. The thickness can be determined manually by the user through a qualitative assessment or automatically using a quantitative measure as an objective function. Minimizing the value of the entropy was selected as the cost function. The effect of the fat layer was simulated as a time delays added to the RF data. Experimental studies addressing that the entropy can be used to accurately determine the thickness of the fat layer depending on the selected region of interest. Images of a six pins phantom were reconstructed using a simple and fast method for digital beamforming.

Keywords – ultrasound imaging, phase aberration, beamforming, image reconstruction.

I. Introduction

Ultrasonic imaging systems have been widely used in medical applications. Techniques using phased array transducers use an array of transducer elements to transmit a focused beam into the body, and each element then becomes a receiver to collect the echoes. The received echoes from each element are dynamically focused to form an image. These systems assume a constant acoustic velocity in the tissue of 1540m/s while steering and focusing the beam. However soft tissues have a range of acoustic velocities that vary from 1470m/s for fat to 1665m/s for collagen [1]. The acoustic wavefront propagation through a region with locally different acoustic velocities will be phase shifted relative to the rest of the wavefront. This effect is known as phase aberration. The effects of phase aberration include a broadening of the point spread function, leading to lower resolution, and increasing the off-axis response, leading to multiple images for the target [2].

The aberator can be modeled as a near field thin phase screen, consistent with the assumption that the layer of subcutaneous fat immediately at the face of the transducer causes the greatest degradation of the beamforming stage [3]. Different techniques have been proposed to correct the phase aberration problem. These techniques are based on measuring and correcting the phase error whether in the time domain or in the frequency domain [4]. These techniques include time delay compensation during the transmission and reception of the ultrasonic beam using different methods, such as adjacent element cross correlation [5], maximum brightness [6], common-mid point methods [7], [8], or through the minimization of the sum of absolute difference (SAD) [9].

All these techniques have common procedures, but there are three different factors distinguish among these different techniques. Each approach attempts to measure deviations from the expected arrival time, or phases, of echo signals received at pairs of elements or element groups on the receiving aperture. The expected arrival times are calculated based on the path length between each element and the focal point and on the expected acoustic velocity of the tissue. Deviation from the expected acoustic velocity distorts the echo signal arrival time profile, resulting in destructive interference of signals and the losses of image quality. Phase correction accounts the distortion by measuring the deviation arrival time profiles and compensating for them in both transmit and receive delays. The distinguishing factors between various correction algorithms are the method of measuring arrival time or phase differences between echo signals, the size and geometric relationship on the receiving aperture, and the method by which measured echo arrival time differences between the elements are combined to generate phase correction profiles.

* Ahmed.ehab@k-space.org

This paper describes a simple method to correct the phase aberration resulted from the thin layer of subcutaneous fat immediately at the face of the transducer. The proposed technique is based on another approach to solve the phase aberration problem. It does not depend on measuring the arrival time differences but it searches for the best thickness of the fat layer which achieves the maximum image quality. This algorithm assumes that the acoustic wave is passing through a uniform distributed fat layer with an acoustic velocity of 1470m/s. Then by determining the thickness of that fat layer, the steering and focusing delays can be calculated accurately by using the velocity of ultrasonic beam in the fat layer, and the velocity of the body tissue for the other layer. By this assumption the distortion arises from using the same velocity for all layers can be eliminated by compensating the focusing and steering delays at each element.

II. METHODS

A. Digital Beamforming

Ultrasonic transducers use an array of piezoelectric elements to transmit a sound pulse into the body and to receive the echoes that return from scattering structures within. This array is often referred to as the imaging system's aperture. The transmit signals passing to, and the received signals passing from the array elements can be individually delayed in time, hence the term phased array because this time shift is equivalent to a phase shift. This is done to electronically steer and focus each sequence of acoustic pulses through the plane or the volume to be imaged in the body. The process of steering and focusing these acoustic pulses is known as beamforming. In this process the time shifts follow a linear pattern across the array from one side to the other side. The uppermost element will be excited first, and an approximately spherical acoustic wavefront will begin propagating from it. A very short time later, the next element will be excited and its wavefront will join the one from the previous element. The sequence will continue until the last element is excited and its wavefront is added to the total. The reciprocity assures that the beam pattern of the receiving mode can be electronically steered using the same linear phase shifts as for the transmitted beam. In the receive mode, the shifted signals are summed together after phase shifting and some signal conditioning to produce a single output.

In this work, receive beamforming only is considered without loss of generality. That is, the beamforming was applied only on the received signals, so the focusing and steering were performed in the receiving mode using N-channel beamformer. The number of channels N is equal to (l_f/F_n) divided by the element width. Where l_f is the depth of focus and F_n is the *f-number* which is considered as an indication for the size of the focal spot [10]. The number of channels N was changed proportional to the depth of focus of each focal point for a fixed F_n equals two.

This reconstruction technique divides the field of view (FOV) into different point targets (raster points), P(i,j), each point represents an image pixel, which are separated laterally and axially by small distances. Each target is considered as a point source that transmits signals to the aperture elements such as in Fig. 1. The beamforming timing is then calculated for each point based on the distance R between the point and the receiving element, and the velocity of ultrasonic beam in the media. Then the samples corresponding to the focal point are synchronized and added to complete the beamforming as the following.

$$P_D(i,j) = \sum_{n=1}^{N} X_n(K_{i,j}) \tag{1}$$

Where P_D (i, j) is the signal value at the point whose its coordinates are (i, j), and X_n ($K_{i,j}$) is the sample corresponding to the target point in the signal X_n received by the element number n. The sample number $K_{i,j}$ which is equivalent to the time delay is calculated using the equation below:

$$K_{i,j} = \frac{R_n(i,j)}{T * c} \tag{2}$$

Where R_n (i, j) is the distance from the center of the element to the point target, c is the acoustic velocity via the media, and T is the sampling period of the signal data.

B. Modeling the fat layer

As mentioned above the problem of phase aberration arises mainly from the false assumption that assumes constant sound velocity over the FOV such as in (2). So the focusing and the steering delays are calculated based on wrong velocities, which will introduce a timing error or phase error. The subcutaneous fat layer participates in this problem, by which the sound velocity propagates in this layer with different velocity equals to 1470m/s [1]. In this paper we propose a simple method that based on modeling the subcutaneous fat layer as a uniform layer at the face of the transducer with a specified thickness F_L such as in Fig. 2. Then by determining the thickness of this layer the delays can be determined accurately. The time delay was divided into two components; the first component is due to the propagation of the ultrasonic waves in the fat layer, so the delay is calculated based on the path length L_f and the velocity of the ultrasonic wave c_f in the fat layer. The second delay component is due to the propagation of the ultrasonic wave through the entire tissue, which is assumed to have the same velocity c, and the delay is calculated based on the path length L_n and the velocity in this tissue, which many systems assumed it to be 1540m/s. The total delay T_t is calculated using the equation below:

$$T_t = \frac{L_f}{c_f} + \frac{L_n}{c} \tag{3}$$

The lengths of L_f and L_n can be determined from the geometry as shown in Fig. 2, and the length L_f can be determined as follow:

$$L_f = \frac{F_L * R_n(i,j)}{l_f} \tag{4}$$

C. Fat Layer Thickness

The determination of the thickness of the subcutaneous fat layer can be made qualitatively by the user or quantitatively by using a simple automatic algorithm. In the first method the user can change the thickness of the fat layer manually from 0mm to 50mm by a specific increment such as 1mm, and the user can determine qualitatively the thickness that achieves the maximum image quality. The second method depends on a simple algorithm that can automatically determine the best thickness of the fat layer that enhances the image quality and decreases the bad effects of the fat layer on the image such as the image blurring. In this research the value of entropy was used as the cost function. Classical entropy-based criteria describe information-related properties for an accurate representation of a given signal. Entropy is a common concept in many fields. The observations reveal that the value of the entropy decreases as the energy distribution within a region of interest (ROI) in the image becomes more precise and has sharper edges, i.e. as the effect of image blurring decreases as the value of the entropy decreases within a specified ROI within the image, or simply the ROI may be the point spread function (PSF). So this algorithm searches for the minimum value of the entropy. The algorithm selects a specific ROI within the image and calculates its value of entropy at different assumed thicknesses for the fat layer. The best thickness for the fat layer will be at the minimum value of entropy. The type of entropy used in this algorithm was the (nonnormalized) Shannon entropy [11], which can be calculated using the following equation:

$$E(s) = -\sum_i s_i^2 \log\left(s_i^2\right) \tag{5}$$

Where s is the signal and $(s_i)_i$ the coefficients of s in an orthonormal basis.

III. RESULTS

The proposed methods were applied to correct real data obtained from the Biomedical Ultrasound Laboratory, University of Michigan. Although the techniques proposed were applied to several data sets, the data set that was used to generate the results in this paper is the one under "Acuson17". The parameters for this data set are as follows: 128 channels, 13.8889 MSPS A/D sampling rate, 3.5 MHz transducer with 0.22mm element spacing, 2048 RF samples per line each represented in 2 bytes, and 8 averages. The data were acquired for a phantom with 6 pins at different positions. The data was used to simulate the N-channel beamformer on receive as discussed above. The radio frequency (RF) signals, A-scans, were recorded from every possible combination of transmitter and receiver for all elements in the 128 element. Fig. 3 shows an example of a typical RF signal that was received. The figure shows 6 peaks which represent the 6 pins of the phantom. A reconstructed image using the N-channel beamformer on receive is shown in Fig. 4. The degradation of the

point spread function (PSF) by increasing the thickness of the fat layer is shown in fig. 5. The degradation of the PSFs is clear, which includes the broadening of the PSF, the decreasing of the magnitude of the main lobe, and the increasing of the magnitude of the side lobes. Fig. 5 (a) represents the PSF of the system with zero fat layer shows a high magnitude and sharp main lobe and small side lobe. The degradation increases with the thickness of the fat layer as shown in Fig. 5 (d), at 3cm fat layer the main lobe decreased, broadened, and the magnitude of the side lobes increased. To test the entropy algorithm, the effect of fat layer was simulated at different thicknesses as a phase delay applied to the original RF data. Then the algorithm was tested to determine the simulated thickness. Fig. 6 shows the changes in the values of the entropy with different fat layer thicknesses. Fig. 6 (a) shows the change of the values of entropy when the simulated fat thickness was 10mm. The minimum value of entropy was at a proposed thickness of 10 mm. In Fig. 6 (b) the same situation happened when the thickness of fat was 20mm, the entropy gave the minimum at 20mm. The thickness of the fat layer was determined by using the entropy of the PSF. Fig. 7 explains an example of the PSFs for the same system before and after the application of the correcting algorithm. Fig. 7 (a) shows a degraded PSF by the effect of 20mm simulated fat layer, and Fig. 7 (b) shows the corrected PSF with its higher main lobe using the entropy to determine the fat thickness that allowing the system to calculate the focusing delay perfectly.

IV. Discussion

The digital beamforming algorithm described is very simple depending on the raster points rather than the radial focal points, so there is no need for the scan conversion from the radial format to the raster format. The beamforming was used to reconstruct the six pin image of the phantom and other images from different datasets. Its performance was limited on displaying larger details in the image, but the beamforming was sufficient to test the phase aberration correction algorithm efficiency. In this study simulation for the beacon refraction was introduced but the reflection effect was neglect so the degradation of the images or the PSFs shown in fig. 5 was mild, so experimental studies will be performed in our next studies. The phase correction algorithm explained previously is very simple. It depends mainly on the determination of the thickness of the subcutaneous fat layer to estimate the focusing delay correctly. The entropy was used as the cost function to estimate the thickness of the fat layer introduces perfect results as shown in Fig. 6 but these results was obtained when a specific ROI in the image was used to calculate the entropy. The accuracy differs totally when another ROI is used. The accuracy was improved when the entropy of various ROIs were added, therefore the error can be reduced. The entropy of the PSF at different thicknesses can be used in the algorithm and then a searching for the minimum entropy value is required. At this minimum value the optimum thickness exists. So in the automatic algorithm for determining the thickness of the fat layer there is no need to reconstruct the whole image, just the values of the entropy of the PSFs can be calculated or a partial area of the image can be reconstructed using the simple beamforming algorithm. After the estimation of the fat layer thickness, the corrected image can be totally reconstructed by the true focusing delays. The simplicity and low computational complexity make this solution very fast, but the main disadvantage is that the accuracy of it is dependent on the selected ROI. Next concerns will focus on this problem and experimental studies will be performed.

V. Conclusions

A fast and accurate correction scheme for the problem of phase aberration in ultrasound images that results from the subcutaneous fat layer is presented. The new method relies on calculating the time delay taking into account the difference in the ultrasonic velocity between the fat and the tissue. So the thickness of the fat layer was determined. The determination of the thickness of the fat layer can be estimated by two methods. The first is manual and the second method is automated based on Shannon entropy as a cost function. Experimental results from both simulations and real data acquired from two different ultrasound systems were used to verify the solution using images reconstructed from a beamforming algorithm applied on receiving mode based on raster points. The results indicate that a significant improvement using the proposed methods and suggest their practicality and clinical utility.

ACKNOWLEDGEMENTS

We would like to thank Dr. Matthew O'Donnell and Biomedical Ultrasonics Laboratory, University of Michigan, Ann Arbor, for making his group's RF data available. We acknowledge also the technical support received from both the International Biomedical Engineering (IBE Technologies), Giza, Egypt, and the Medical Equipment Calibration Lab (MECL), Cairo University, Giza, Egypt.

REFERENCES

[1] S.A. Gross, R.L. Johnston, and F. Dunn, "Comprehensive compilation of empirical ultrasonic properties of mammalian tissues, "*J. Acoustic. Soc. Amer.*, vol. 64, pp. 423-457,1978.

[2] G.C. Ng, S.S. Worrell, P. D. Freiburgger, and G. E. Trahey, "A comparative evaluation of several phase aberration correction algorithms," *IEEE Trans. Ultrason., Ferroelec. Freq. Contr.* , vol. 41, no. 5, pp. 631-643, 1994.

[3] G. C. Ng. P. D. Freiburgger, W. F. Walker, and G. E. Trahey, " A speckle Target Adaptive Imaging Technique in the presence of distributed aberration," *IEEE Trans. Ultrason., Ferroelec. Freq. Contr.* , vol. 44, no. 1, pp. 140-151, 1997.

[4] Z. Farouk, A. M. Youssef, and Y. M. Kadah "Successive optimization for fast aberration correction," *Proc. SPIE Medical Imaging 2003*, San Diego , 2003.

[5] S. W Flax and M. O'Donnell," Phase aberration correction using signals from point reflectors and diffuse scatterers: basic principles," *IEEE Trans. Ultrason., Ferroelec. Freq. Contr.* , vol. 35, no. 6, pp. 758-767, 1988.

[6] L. F. Nock, G. E. Trahey, and S.W. Smith, " Phase aberration correction in medical ultrasound using speckle brightness as a quality factor," *J. Acoust. Soc. Am.*, vol. 85, no. 5, pp. 1819-1833, 1989.

[7] D. Rachlin, " Direct estimation of aberration delays in pulse-echo imaging systems," *J. Acoust. Soc. Am.*, vol. 88, no. 1, pp. 191-198, 1990.

[8] Y. Li, " Phase aberration correction algorithm using near-field signal redundancy method: algorithm," *Ultrason. Imag.*, vol. 17, no. 1, pp. 64, 1995.

[9] M. Karaman, A. Atalar, H. Koymen, M. O'Donnell, "A phase aberration correction method for ultrasound imaging," *IEEE Trans. Ultrason., Ferroelec. Freq.* Contr. , vol. 40, no. 4, pp. 275-282, 1993.

[10] D. A. Christensen, *Ultrasonic Bioinstrumentation*, New York: Wiley, 1988.

[11] Coifman, R.R., M.V. Wickerhauser, "Entropy-based Algorithms for best basis selection," *IEEE Trans. on Inf. Theory*, vol. 38, no. 2, pp. 713-718, 1992.

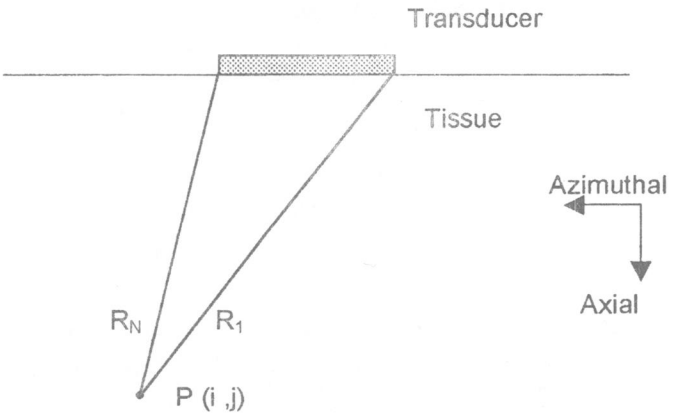

Fig. 1. The FOV is divided into point targets P (i,j). Each point target is considered as a virtual source transmitting acoustic waves to each element in the aperture.

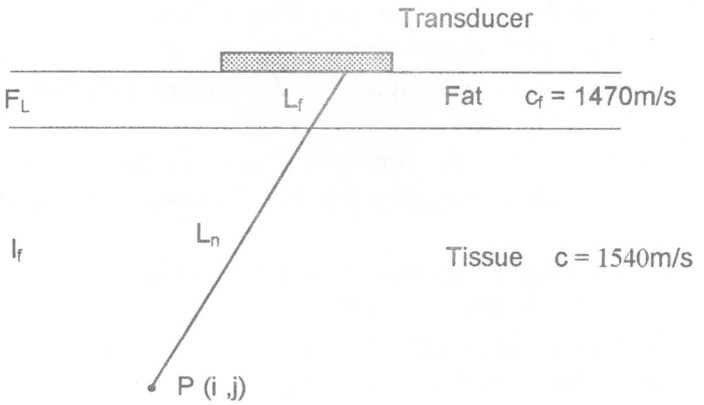

Fig. 2. The path of the ultrasonic beam from the point target P at depth of focus l_f to an aperture element through the tissue layer and the fat layer of thickness F_L.

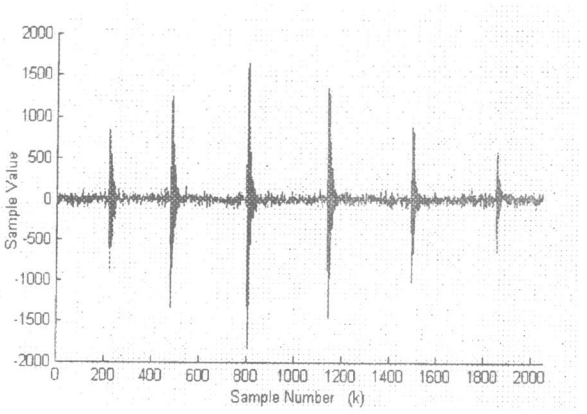

Fig. 3. Typical RF signal for the phantom shows the six peaks of the phantom pins.

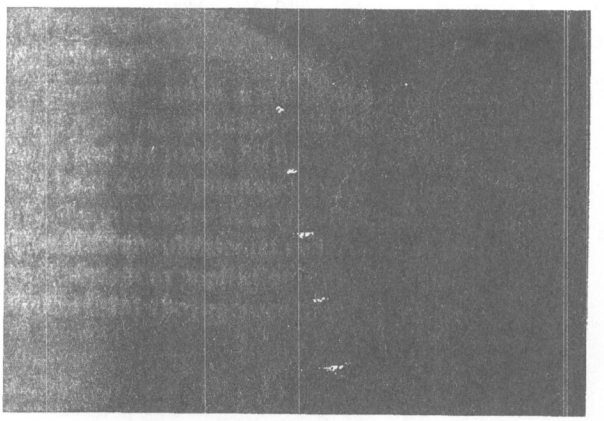

Fig. 4. Ultrasound image of the phantom reconstructed by receive beamforming using the raster focal points technique.

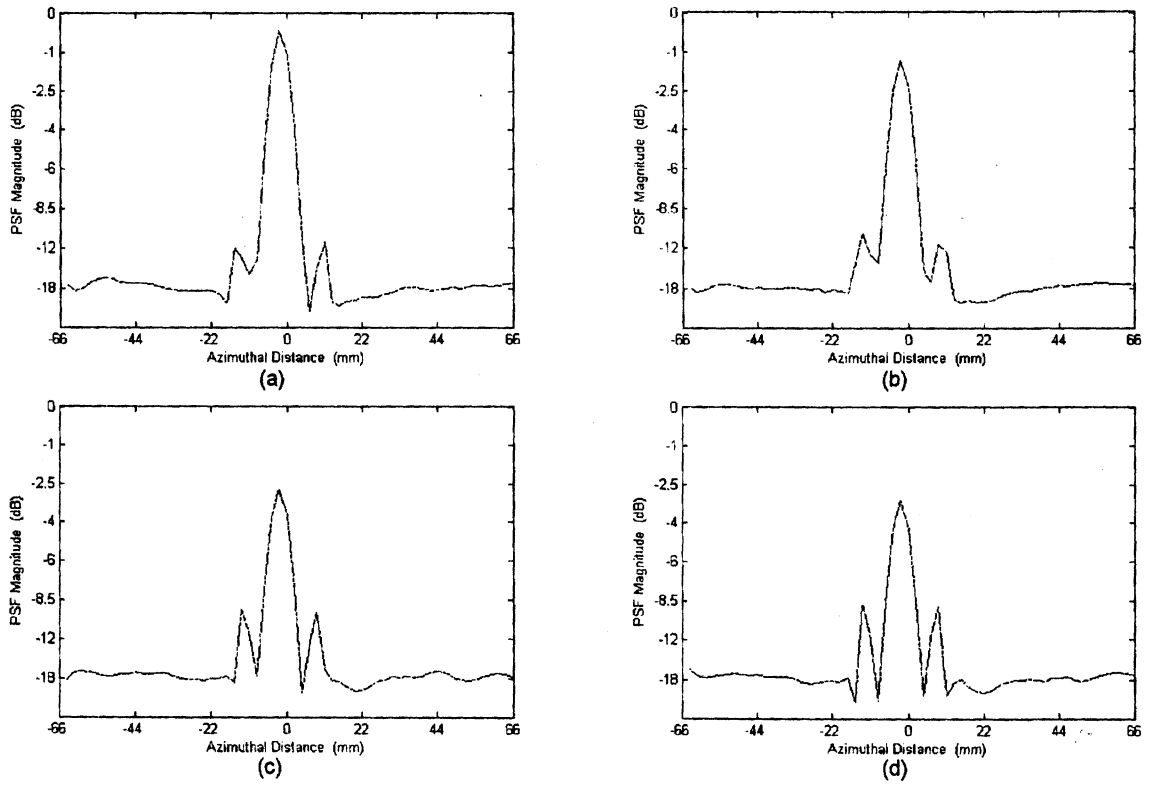

Fig. 5. Two dimensional point spread function at different thicknesses for the simulated subcutaneous fat layer: (a) 0mm, (b) 1cm, (c) 2cm, and (d) 3cm.

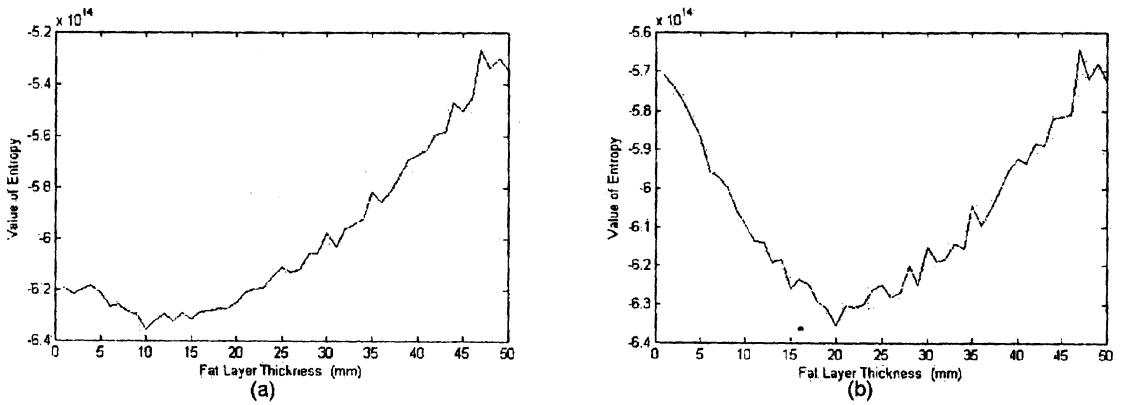

Fig. 6. The changes of the value of the entropy with the assumed thicknesses of the fat layer: (a) at 10mm fat layer, and (b) at 20mm fat layer.

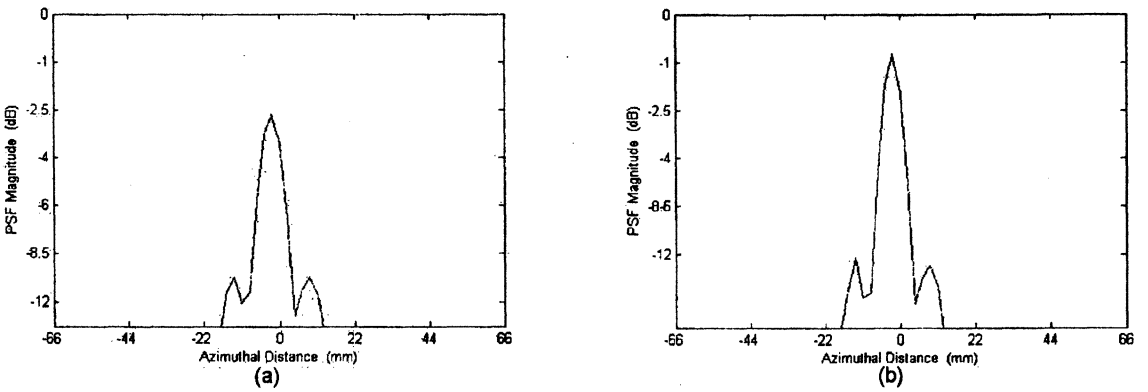

Fig. 7. Aberrated and corrected PSF: (a) Aberrated PSF by 20mm fat layer, and (b) corrected PSF